

AD-A073093

# Technical Note

1979-48

K.P. Dunn

## Accuracy of Parameter Estimates for Closely Spaced Optical Targets

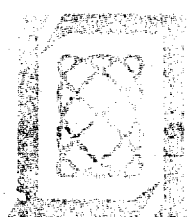
13 June 1979

Prepared for the Department of the Army  
under Electronic Systems Division Contract F19628-78-C-0602 by

**Lincoln Laboratory**

MASSACHUSETTS INSTITUTE OF TECHNOLOGY

LEXINGTON, MASSACHUSETTS



Approved for public release; distribution unlimited.

BEST AVAILABLE COPY  
BEST AVAILABLE COPY

The work reported in this document was performed at Lincoln Laboratory,  
a center for research operated by Massachusetts Institute of Technology.  
This program is sponsored by the Ballistic Missile Defense Program Office,  
Department of the Army; it is supported by the Ballistic Missile Defense  
Advanced Technology Center under Air Force Contract F19628-79-C-0002.

This report may be reproduced to satisfy needs of U.S. Government agencies.

The views and conclusions contained in this document are those of the  
contractor and should not be interpreted as necessarily representing the  
official policies, either expressed or implied, of the United States  
Government.

This technical report has been reviewed and is approved for publication.

FOR THE COMMANDER

*Joseph C. Sylek*  
Joseph C. Sylek  
Project Officer  
Lincoln Laboratory Project Office

BEST AVAILABLE COPY

MASSACHUSETTS INSTITUTE OF TECHNOLOGY  
LINCOLN LABORATORY

ACCURACY OF PARAMETER ESTIMATES  
FOR CLOSELY SPACED OPTICAL TARGETS

K-P. DUNN

Group 32

TECHNICAL NOTE 1979-43

13 JUNE 1979

AUG 27 1979

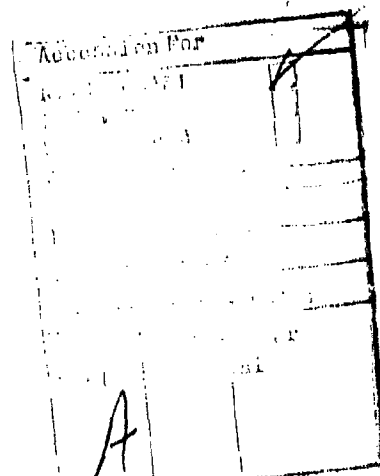
Approved for public release; distribution unlimited.

LEXINGTON

MASSACHUSETTS

## ABSTRACT

Cramer-Rao lower bounds on the degradation of measurement precision for closely spaced optical targets are found. Degradation is more severe than previously thought, especially, for small target separations. The bound obtained by a previous analysis, is, in fact, theoretically identical to the Cramer-Rao bound presented here. The disagreement in results is caused by numerical problems in a computer program used in the previous analysis.



CONTENTS

I.	INTRODUCTION	1
II.	ANALYSIS	4
III.	NUMERICAL RESULTS	10
IV.	SUMMARY AND CONCLUSION	19
	APPENDIX	26
	ACKNOWLEDGMENTS	30
	REFERENCES	31

## I. INTRODUCTION

During the past several years considerable attention has been focused upon the accuracy of parameter estimates for optically unresolved objects [1] - [4]. A review of the literature shows that predictions for the variances of the parameter estimates are obtained via different analytical approaches using different assumptions on the noise environments. In [1], a particular "resolution scale" is proposed in order to relate the resolution capability of a sensor with its measurement precision degradation factor due to multi-target interference. Similar studies have been made for radar system applications, see for example [5] and [6]. It is, moreover, pointed out in [5] that a complete analysis of the resolution problem requires extensive simulation and that the resulting error probabilities may depend heavily upon the choice of the detection as well as the estimation scheme. The criterion for resolving two closely spaced radar targets appears to be somewhat arbitrary. In [6], for example, it is defined as twice the value of the angular accuracy of the weaker target. Similar measures have also been used in the optical community. It is outside the scope of this report to discuss the merits of various resolution criteria in a more extensive manner. It is, however, important to point out that using parameter estimation performance degradation results from [1] - [4], or other similar works, to predict the resolution capability of some other specific sensor system without extensive simulation can be misleading. The casual use of numerical

results from these works could lead to false conclusions about the sensor capability.

In [1] - [4], theoretical lower bounds on the variances of various parameters associated with the target intensities and angular positions have been derived. The bounds presented in [2] - [4] are Cramer-Rao lower bounds. Different pulse shapes and sensor noise models are considered and compared. The results presented in [1] are obtained using a different error analysis technique and, furthermore, the parameters to be estimated are different from those considered in [2] - [4]. Attempts have been made by Miller [2] to compare results obtained from these two different techniques and problem formulations. Unfortunately, Miller could not achieve agreement between the numerical results nor explain the disagreements. Miller's predicted degradation of the parameter estimation performance was much more severe than that presented by Fried [1], particularly for target separations much less than the optical diffraction limit. Surprisingly good estimation performance was predicted in [1] for small target separations. These results have been used on several occasions for predicting resolution capability of certain optical system. For this reason we felt it important to establish the cause of the discrepancies reported in [2].

As discussed in [2], although the problem formulations are quite different in [1] and [2], they should produce results which are comparable. The two analysis differ in the choice of optical

pulse shape but we do not believe that this alone could be the cause of the drastic discrepancies observed in [2]. The purpose of this report is to establish the cause of the above-mentioned disagreement. Our analysis has shown that the two approaches although superficially different are in fact identical analytically. We can demonstrate that the differences in results are caused by numerical problems which exist in one of the computer programs used in [1].

In the next section, the Cramer-Rao bounds are derived for the problem formulated by Fried [1]. A detailed derivation which established that the equations in [1] are in fact Cramer-Rao bounds may be found in the Appendix. In Section III, the cause of the numerical problems in [1] is discussed and illustrated by a particular example. Results of some typical cases considered in [1] are presented and compared. A summary and conclusions are given in Section IV.

## III. ANALYSIS

Let us assume that  $p(t)$  is the output of an optical sensor to a unit strength point source such that

$$\int_{-\infty}^{\infty} p^2(t) dt = 1. \quad (1)$$

The problem treated here concerns the measurement of a pair of point sources with relative strength  $(1+\frac{1}{4}\Delta):(1-\frac{1}{4}\Delta)$ , separation  $T$  and the location of the midpoint between them at  $t_0$ . The output of the sensor becomes<sup>†</sup>

$$s(t) = a(1+\frac{1}{4}\Delta)p(t-t_0+\frac{1}{4}T) + a(1-\frac{1}{4}\Delta)p(t-t_0-\frac{1}{4}T) \quad (2)$$

where  $a$  is the average strength of the point sources which does not appear in the problem formulation given in [1].<sup>††</sup> We wish to determine these parameters from a noisy measurement taken at the output of the sensor

$$y(t) = s(t) + n(t) \quad (3)$$

where  $n(t)$  is white Gaussian noise with two-sided

<sup>†</sup>For easier comparison with results presented in [1], we adopt the notation used in [1].

<sup>††</sup>For the analysis presented in [1], the value of  $a$  is not important. The reason for having it in Eq. (2) will become clear in later discussions.

power spectrum density  $N_0/2$ .

Let  $\rho(t)$  be the autocorrelation function of  $p(t)$ , i.e.

$$\rho(t) \triangleq \int_{-\infty}^{\infty} p(\tau)p(\tau-t)d\tau \quad (4)$$

and  $\rho(0)=1$ . The Cramer-Rao lower bound on the variance of any unbiased estimator of the unknown parameters: relative strength,  $R = (1 - \frac{1}{4}\Delta) / (1 + \frac{1}{4}\Delta)$ , separation,  $T$ , midpoint,  $t_0$ , can be obtained by inverting the Fisher information matrix,  $F$ , whose  $(i,j)$ th element is:<sup>[7]</sup>

$$F_{ij} = E \left\{ \frac{\partial \ln \Lambda}{\partial \alpha_i} \frac{\partial \ln \Lambda}{\partial \alpha_j} \right\} \quad (5)$$

where  $E\{ \}$  denotes statistical expectation and  $\alpha_i$  denotes the  $i^{\text{th}}$  unknown parameter, namely,  $\alpha_1=R$ ,  $\alpha_2=T$ ,  $\alpha_3=t_0$  and  $\alpha_4=a$ , and where  $\ln \Lambda$  is the log likelihood ratio [7, p. 274]

$$\ln \Lambda = \frac{1}{N_0} \left\{ 2 \int_{-\infty}^{\infty} y(t)s(t)dt - \int_{-\infty}^{\infty} s^2(t)dt \right\}. \quad (6)$$

Substituting (6) into (5), we have

$$F_{ij} = \frac{2}{N_0} \left\{ \int_{-\infty}^{\infty} \left( \frac{\partial s(t)}{\partial \alpha_i} \right) \left( \frac{\partial s(t)}{\partial \alpha_j} \right) dt \right\} \quad (7)$$

where

$$\frac{\partial s(t)}{\partial R} = \frac{1}{2}a(1+\frac{1}{2}\Delta)^2 [p(t-t_0-\frac{1}{2}\Delta) - p(t-t_0+\frac{1}{2}\Delta)] \quad (8a)$$

$$\frac{\partial s(t)}{\partial T} = \frac{1}{2}a \left[ (1+\frac{1}{2}\Delta)\dot{p}(t-t_0+\frac{1}{2}\Delta) - (1-\frac{1}{2}\Delta)\dot{p}(t-t_0-\frac{1}{2}\Delta) \right] \quad (8b)$$

$$\frac{\partial s(t)}{\partial t_0} = -a \left[ (1+\frac{1}{2}\Delta)\dot{p}(t-t_0+\frac{1}{2}\Delta) + (1-\frac{1}{2}\Delta)\dot{p}(t-t_0-\frac{1}{2}\Delta) \right] \quad (8c)$$

$$\frac{\partial s(t)}{\partial a} = (1+\frac{1}{2}\Delta)p(t-t_0+\frac{1}{2}\Delta) + (1-\frac{1}{2}\Delta)p(t-t_0-\frac{1}{2}\Delta) \quad (8d)$$

and  $\dot{p}(t)$  is the 1<sup>st</sup> order derivative of  $p(t)$  with respect to  $t$ . Then the elements of the Fisher information matrix (Eq. (7)) are:

$$F_{11} = a^2(1+\frac{1}{2}\Delta)^4 [1-p(T)]/N_0 \quad (9a)$$

$$F_{12} = \frac{1}{2}\Delta a^2(1+\frac{1}{2}\Delta)^2 \dot{p}(T)/N_0 \quad (9b)$$

$$F_{13} = -2a^2(1+\frac{1}{2}\Delta)^2 \dot{p}(T)/N_0 \quad (9c)$$

$$F_{14} = -\Delta a(1+\frac{1}{2}\Delta)^2 [1-p(T)]/N_0 \quad (9d)$$

$$F_{22} = a^2 [(1-\frac{1}{2}\Delta)^2 \ddot{p}(T) - (1+\frac{1}{2}\Delta)^2 \ddot{p}(0)]/N_0 \quad (9e)$$

$$F_{23} = 2\Delta a^2 \dot{p}(0)/N_0 \quad (9f)$$

$$F_{24} = 2a(1-\frac{1}{4}\Delta^2)\dot{\rho}(T)/N_0 \quad (9g)$$

$$F_{33} = -4a^2[(1-\frac{1}{4}\Delta^2)\ddot{\rho}(T) + (1+\frac{1}{4}\Delta^2)\dot{\rho}(0)]/N_0 \quad (9h)$$

$$F_{34} = 0 \quad (9i)$$

$$F_{44} = 4[(1+\frac{1}{4}\Delta^2) + (1-\frac{1}{4}\Delta^2)\rho(T)]/N_0 \quad (9j)$$

where  $\dot{\rho}$  and  $\ddot{\rho}$  are the 1<sup>st</sup> and 2<sup>nd</sup> order derivatives of  $\rho$ , respectively.

In principle, one can invert this  $4 \times 4$  symmetric matrix,  $F$ , directly to find the lower bounds on the variance of the parameter estimates for particular values of  $R$ ,  $T$ ,  $t_0$  and  $a$ . If  $a$  is not a parameter of interest, we can also invert an equivalent  $3 \times 3$  matrix,  $\bar{F}$ , associated with  $R$ ,  $T$  and  $t_0$ .  $F$  can be obtained from  $\bar{F}$  by applying the matrix inversion formula for a partitioned matrix as below:

$$\bar{F} = F_1 - F_2^T F_{44}^{-1} F_2 \quad (10)$$

where  $F_1$  is the upper left  $3 \times 3$  matrix of  $F$ ,  $F_2$  is the 1<sup>st</sup> three elements of the 4<sup>th</sup> row of  $F$ . Therefore the elements of  $\bar{F}$  can be written:

$$\bar{F}_{11} = 4a^2(1+\frac{1}{4}\Delta)^4(1-\rho^2(T))/F_0 \quad (11a)$$

$$F_{12} = 4\Delta a^2 (1+\frac{1}{2}\Delta)^2 \rho(T) / F_0 \quad (11b)$$

$$F_{13} = -2a^2 (1+\frac{1}{2}\Delta)^2 \rho(T) / N_o \quad (11c)$$

$$\bar{F}_{22} = a^2 [(1-\frac{1}{2}\Delta^2)\rho(T) - (1+\frac{1}{2}\Delta^2)\rho(0)] / N_o - 4(a(1-\frac{1}{2}\Delta^2)\rho(T))^2 / F_0 \quad (11d)$$

$$\bar{F}_{23} = 2\Delta a^2 \rho(0) / N_o \quad (11e)$$

$$\bar{F}_{33} = -4a^2 [(1-\frac{1}{2}\Delta^2)\rho(T) + (1+\frac{1}{2}\Delta^2)\rho(0)] / N_o \quad (11f)$$

and  $F_0 = N_o^2 F_{44}$ . (11g)

The lower bounds on the variances of the estimates for R, T, and  $t_o$  are:

$$\text{CRB } (R) = (\bar{F})^{-1}_{11}, \quad (12a)$$

$$\text{CRB } (T) = (\bar{F})^{-1}_{22}, \quad (12b)$$

$$\text{CRB } (t_o) = (\bar{F})^{-1}_{33}. \quad (12c)$$

The relative measurement precision defined in [1] can be written as the following:<sup>†</sup>

$$F_\Delta(T) \triangleq \left[ \frac{\text{CRB}(R)_{T=\infty}}{\text{CRB}(R)} \right]^{\frac{1}{2}} \quad (13a)$$

<sup>†</sup>The relative measurement precision is the reciprocal of the degradation factor presented in [2]-[4]. The estimation performance degrades as the value of the relative measurement precision decreases.

$$F_T(T) \triangleq \left[ \frac{\text{CRB}(T)_{T=\infty}}{\text{CRB}(T)} \right]^{\frac{1}{2}} \quad (13b)$$

$$F_t(t_0) \triangleq \left[ \frac{\text{CRB}(t_0)_{T=\infty}}{\text{CRB}(t_0)} \right]^{\frac{1}{2}} \quad (13c)$$

where  $\text{CRB}(R)_{T=\infty}$ ,  $\text{CRB}(T)_{T=\infty}$  and  $\text{CRB}(t_0)_{T=\infty}$  can be obtained by inverting  $F$  for  $T=\infty$ . It is obvious that  $\rho(\infty)=\delta(\infty)=\dot{\rho}(\infty)=0$ , then we have

$$\text{CRB}(R)_{T=\infty} = N_0 [1+\frac{1}{4}\Delta^2] / a^2 [1+\frac{1}{4}\Delta]^4, \quad (14a)$$

$$\text{CRB}(T)_{T=\infty} = -N_0 [1+\frac{1}{4}\Delta^2] / a^2 [1-\frac{1}{4}\Delta^2]^2 \rho(0), \quad (14b)$$

and

$$\text{CRB}(t_0)_{T=\infty} = \frac{1}{4} \text{CRB}(T)_{T=\infty}. \quad (14c)$$

From Eqs. (11a)-(11f) and (14a)-(14c), it can be seen easily that the degradation factors  $F_A$ ,  $F_T$  and  $F_t$  are in fact independent of the value of  $a$ . This independence has also been observed in [2]-[4] for the additive white Gaussian sensor noise model. It should be noted that the actual estimation performances of the estimators of  $R$ ,  $T$  and  $t_0$  are not independent of target intensity  $a$ , this can be seen easily from the expression of the CRB's.

The autocorrelation function  $\rho(t)$  and its derivatives do not appear specifically in the expressions for  $F_A$ ,  $F_T$  and  $F_t$  in [1].

It is not difficult to show that they are actually related to the functions defined in [1], namely:

$$\rho(T) = G_0(T), \quad (15)$$

$$\dot{\rho}(T) = -2\pi H_1(T), \quad (16)$$

and

$$\ddot{\rho}(T) = - (2\pi)^2 G_2(t). \quad (17)$$

With the help of Eqs. (15)-(17), one should be able to show that the degradation factors given in Eqs. (13a)-(13c) are in fact identical to those presented in [1]. The proof will be given in the Appendix.

### III. NUMERICAL RESULTS

We find that the numerical values of  $F_A$ ,  $F_T$  and  $F_t$  calculated via Eqs. (13a)-(13c) using values of  $G_0$ ,  $G_2$  and  $H_1$  provided in Table 1 of [1] are identical to values of  $F_A$ ,  $F_T$  and  $F_t$  in Table 3 of [1]. This proves that the analytical results of [1] and the Cramer-Rao bounds derived in the previous section are identical. However, this does not explain the reason for discrepancies between the results presented in [1] and [2]. After we employ the auto-correlation function of the pulse shape used in [2], that is:<sup>+</sup>

$$\rho(T) = 6(aT - \sin aT)/a^3 T^3 \quad (18)$$

<sup>+</sup>This is a pulse shape suggested by Fried [1, Eq. (72)] as a good approximation to the pulse shape considered in [1].

with  $\alpha=1.6\pi$ , we are able to regenerate results presented in [2] by using the computer program given in [1] - a program which calculates  $F_A$ ,  $F_T$  and  $F_t$  from a given set of values of  $G_0$ ,  $G_2$  and  $H_1$ . It is quite obvious that the discrepancies discussed in [2] are merely numerical problems which exist in the program for the calculation of  $G_0$ ,  $G_2$  and  $H_1$ . It is found that in that program of reference [1] the following formulas were used:

$$\sin(T+\Delta T) = \sin T \cos \Delta T + \cos T \sin \Delta T \quad (19a)$$

$$\cos(T+\Delta T) = \cos T \cos \Delta T - \sin T \sin \Delta T \quad (19b)$$

for numerical integration (Simpson's rule) of  $G_0$ ,  $G_2$  and  $H_1$ . Interpolation of sine and cosine functions via Eqs. (19a), (19b) may often have numerical inaccuracy, especially, when these functions are evaluated at multiples of  $\pi^*$ . We believe this to be the cause of numerical problem observed in [1], when the target separation is  $2.44 \lambda/D$ . In order to show the effects of such interpolation errors on results in [1], we selected a pulse shape such that the analytical expressions for  $G_0$ ,  $G_2$  and  $H_1$  can be obtained. The pulse shape having autocorrelation function given in (18) is used. The numerical errors for  $G_0$ ,  $G_2$  and  $H_1$  are shown in Figure 1 for this particular pulse shape. Although the percentage errors on the values of  $G_0$ ,  $G_2$  and  $H_1$  do not appear significant, they are large enough to create severe discrepancies in the bound

\*The actual fault in the calculation is not these formulas, but the programming error that updates the value of  $\sin T$  by  $\sin(T+\Delta T)$  before calculating (19b).

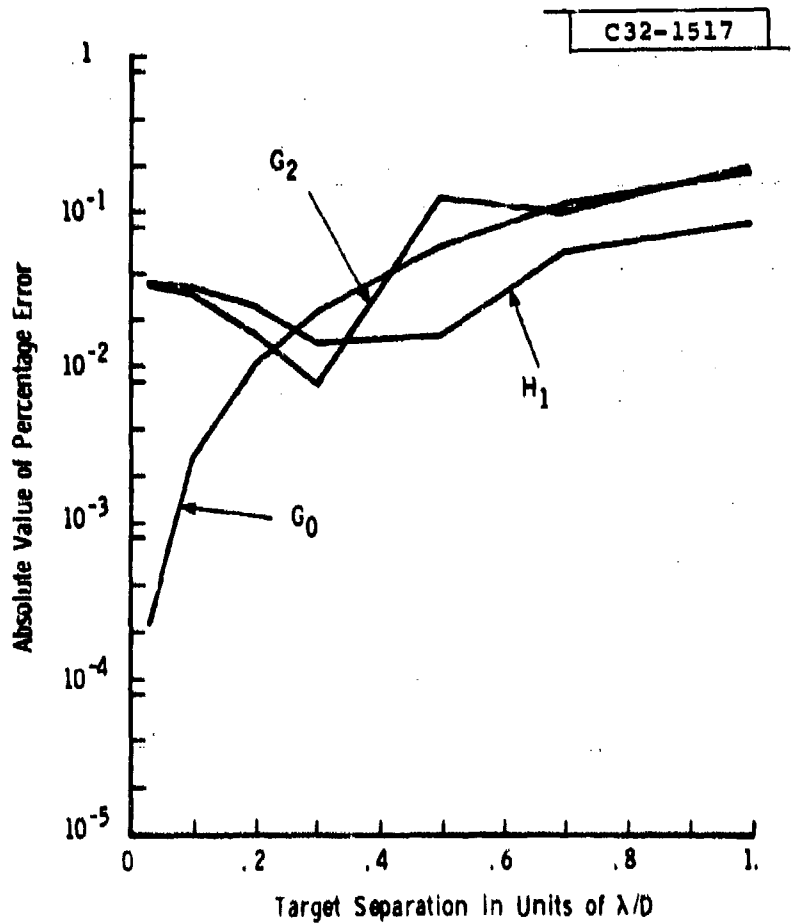


Fig.1. Absolute value of numerical errors for  $G_0$ ,  $G_2$  and  $H_1$  using computer program used in [1] for pulse shape having autocorrelation function given in Eq.(18).

computations. It is easiest to see the difference in the value of the determinant of the covariance matrix

$$V \triangleq \text{cov}[\delta t_0, \delta T, \delta \Delta] \quad (20)$$

computed via interpolation and exact values of  $G_0$ ,  $G_2$  and  $H_1$ . The square roots of the ratios of these determinants are plotted against target separation in Figure 2. It indicates that there are severe discrepancies in the values of these determinants, especially when the target separation is small.

In the rest of this report only the pulse shape presented in [1] will be considered. Figure 3 is a comparison of results obtained by the method of this report to results presented in [1] and [2]. As expected, results obtained from the current analysis, or from the numerical integration with exact values of sines and cosines, are much closer to those obtained via the approximate pulse shape presented in [2]. It is interesting to notice that the difference between current results and results presented in [1] is proportional to the ratio of the square root of the determinants illustrated in Figure 2.

Results of  $F_\Delta$ ,  $F_T$  and  $F_t$  for a detector width equal to  $2.0 \lambda/D$  from the current analysis are shown in Figs. 4, 5 and 6, respectively. Values of  $F_\Delta$ ,  $F_T$  and  $F_t$  presented in [1] are plotted for comparison. We notice that a similar trend of disagreement is repeated here. For separation much less than  $\lambda/D$ ,

C32-1518

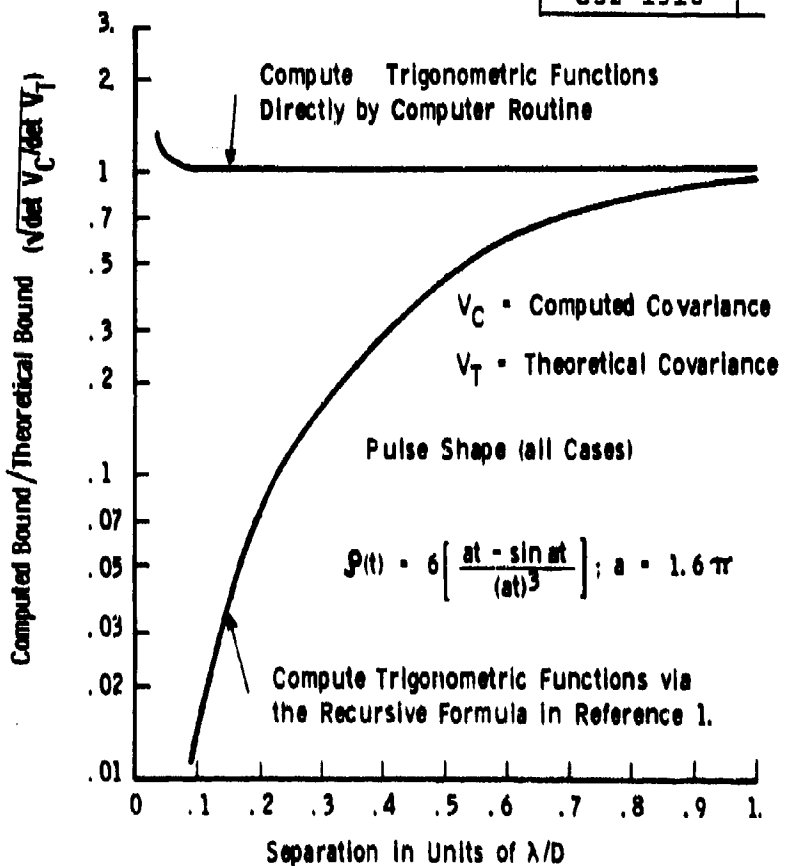


Fig.2 Relative error in the bound computation for different ways of calculating trigonometric functions.

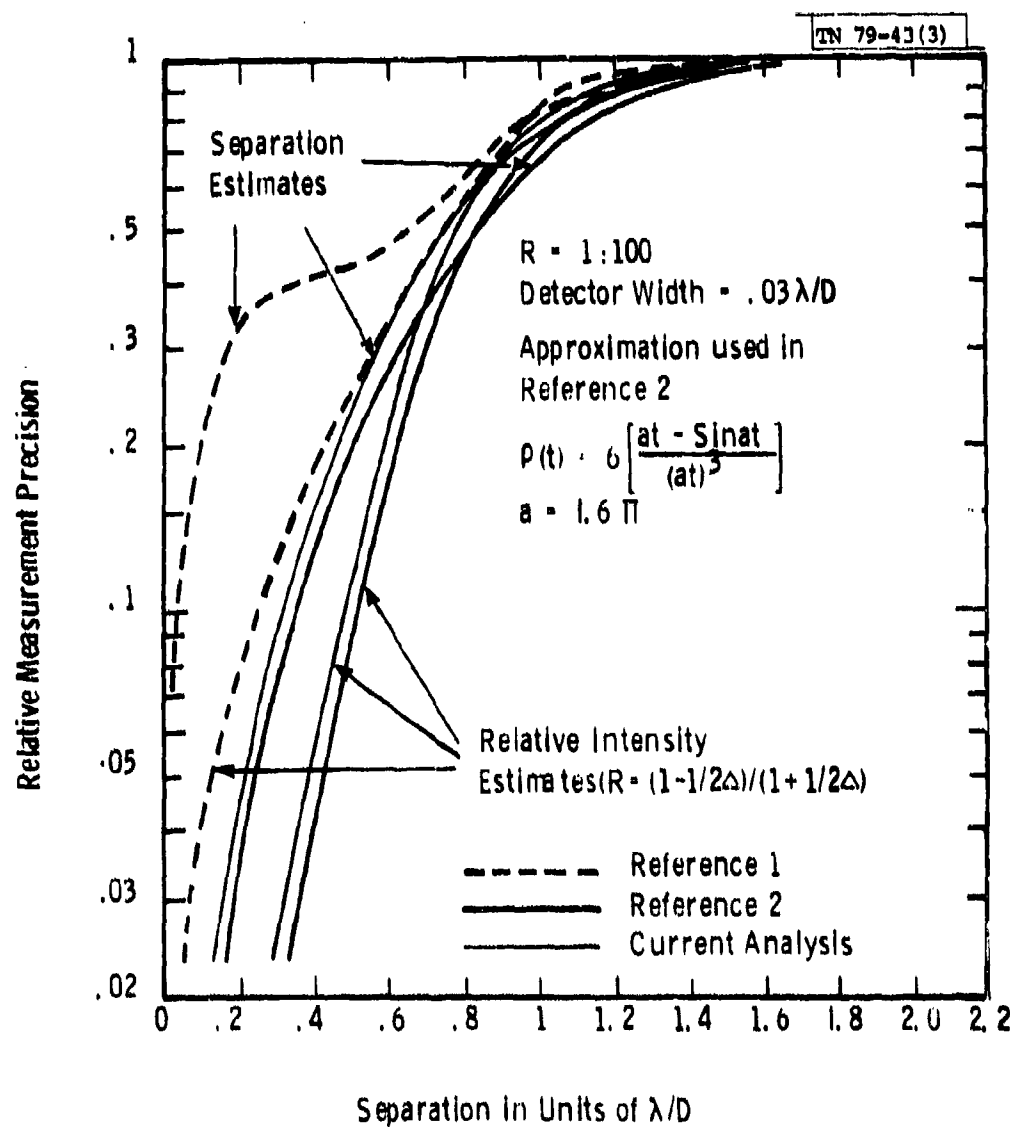


Fig. 3 A comparison of results obtained by current analysis to results presented in [1] and [2]. Notice that the results obtained by current analysis are much closer to those obtained in [2], where an approximated pulse shape was used. The relative measurement precision is the reciprocal of the degradation factor presented in [2]-[4].

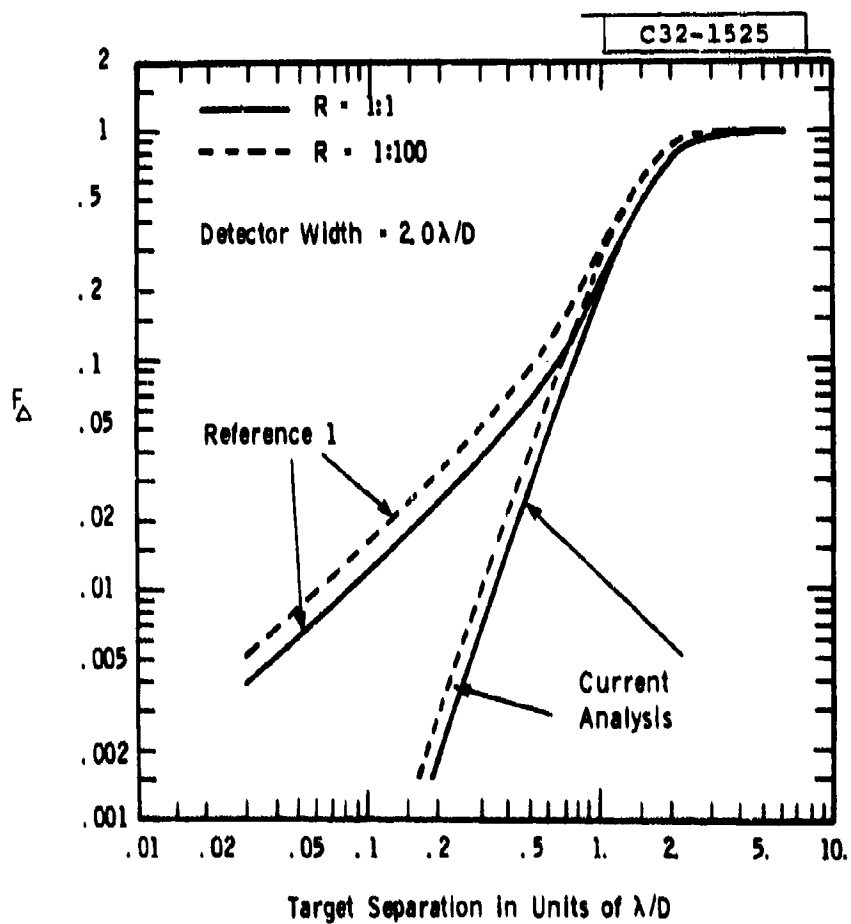


Fig.4 A comparison of values of  $F_A$ , the relative intensity measurement precision, obtained by current analysis to those presented in [1] for detector width equals  $2.0 \lambda/D$ . Two different intensity ratios are considered.

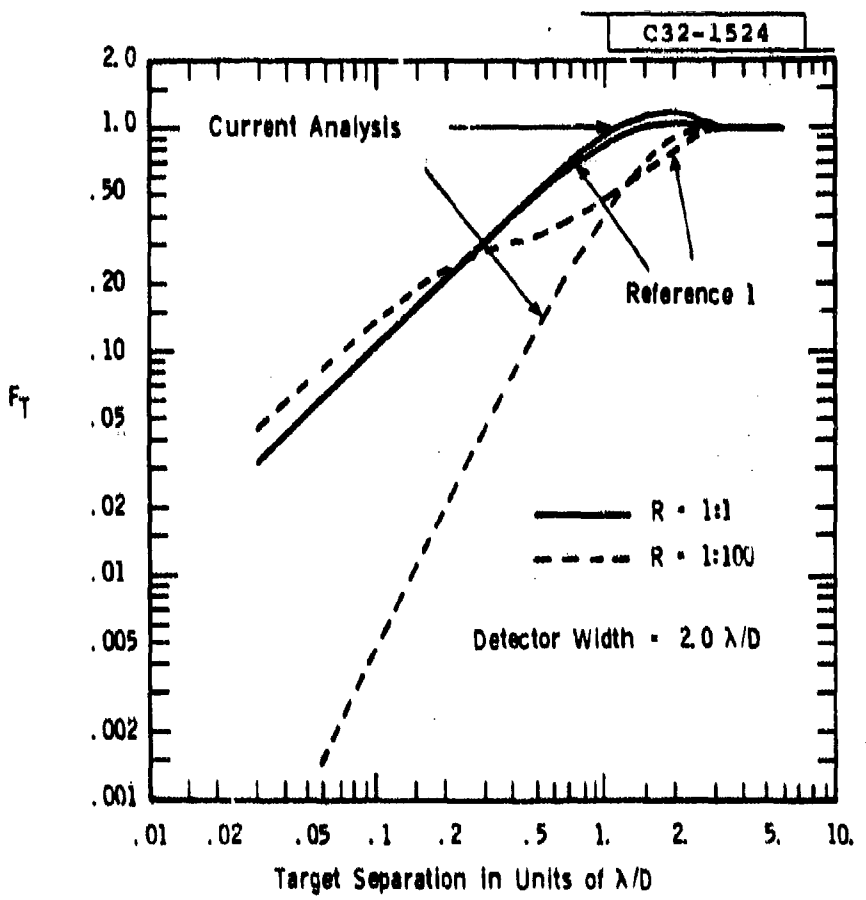


Fig. 5 A comparison of values of  $F_T$ , the relative separation measurement precision, obtained by current analysis to those presented in [1].

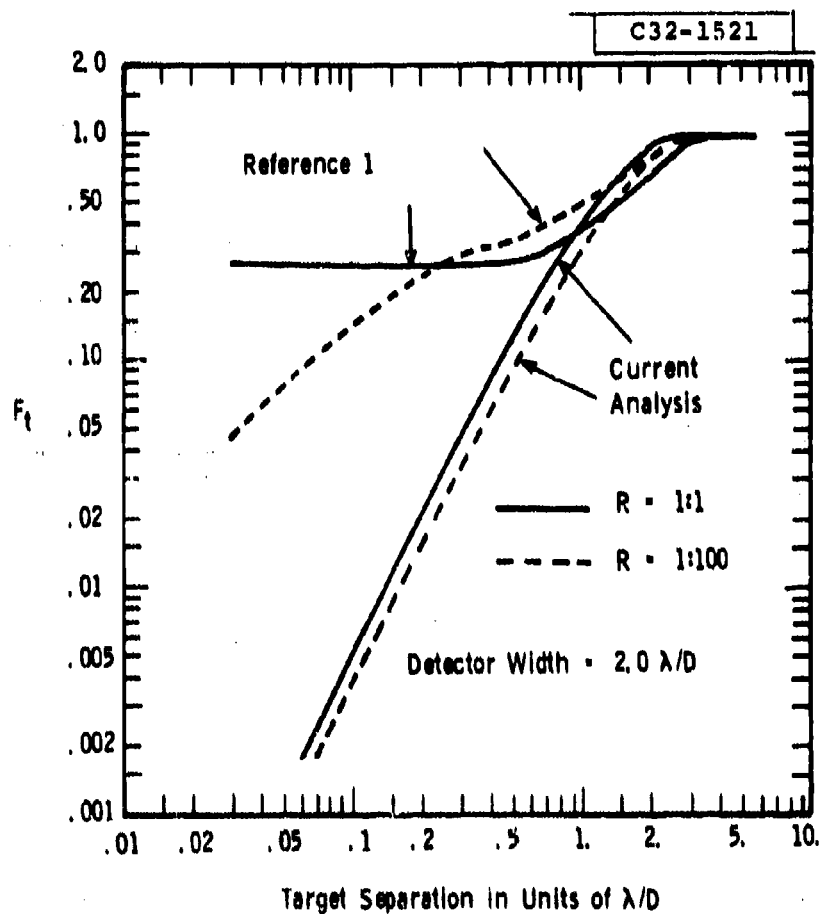


Fig.6 A comparison of values of  $F_t$ , the relative midpoint location measurement precision obtained by current analysis to those presented in [1].

the value of  $F_A$ ,  $F_T$  and  $F_t$  can differ by as much as 3 orders of magnitude! This severe discrepancy can change the conclusions regarding the capability of an optical sensor system drastically.

In Figures 7 through 9, values of  $F_A$ ,  $F_T$  and  $F_t$  are plotted against target separation for detector widths equal to  $0.3\lambda/D$ ,  $2.44\lambda/D$  and  $10\lambda/D$ , respectively. Although the values of  $F_A$ ,  $F_T$  and  $F_t$  are very different from those in [1] for smaller target separation, the target separation corresponding to  $F_A=0.5$  (3dB degradation) does not change a lot due to the numerical errors. Figure 10 shows the value of target separation for  $F_A=0.5$  and the "resolution scale" defined in [1] as a function of the detector width. It indicates that regardless of the numerical problem presented in [1] for small target separation, the central result of [1] concerning about the proposed resolution scale is still valid.

#### IV. SUMMARY AND CONCLUSION

The degradation of estimates of relative target strength, target separation, and midpoint position for a pair of closely spaced objects can be assessed via the method presented here. We also show that the results presented in [1] and [2], which have numerical disagreements, are in fact theoretically identical. The cause of the discrepancy reported in [2] is due to numerical problems occurring in a computer program used by Fried. The rms precision with which we can measure the location of the midpoint

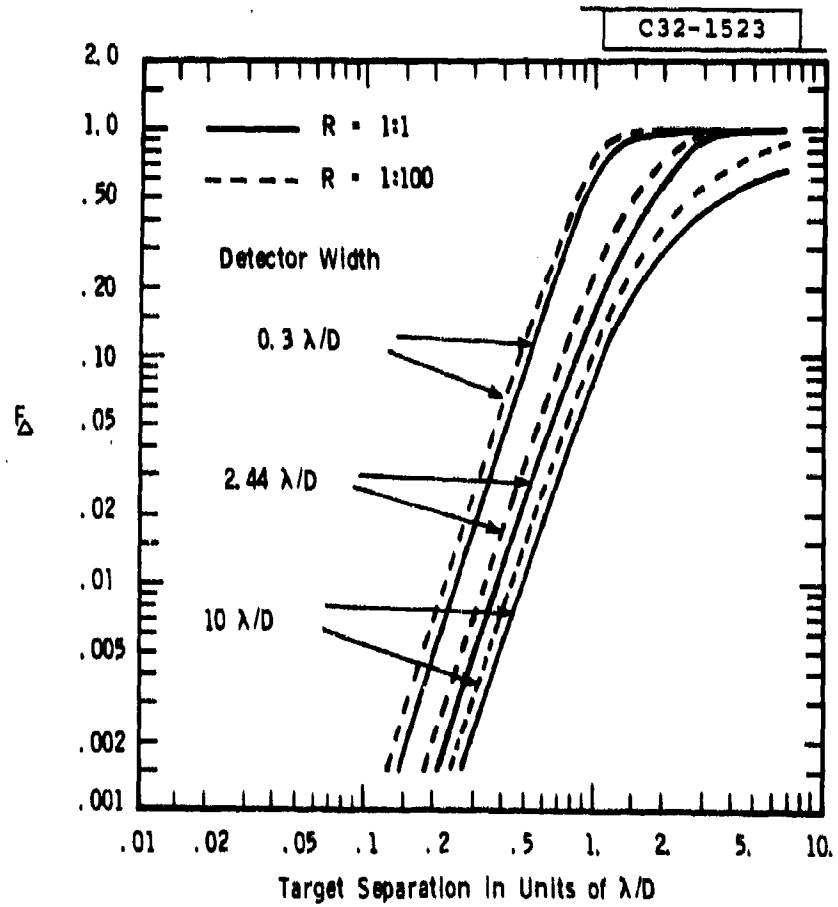


Fig. 7 Degradation of measurement precision on the target relative intensity as a function of target separation. Results are shown for detector widths equal to  $0.3\lambda/D$ ,  $2.44\lambda/D$  and  $10\lambda/D$ .

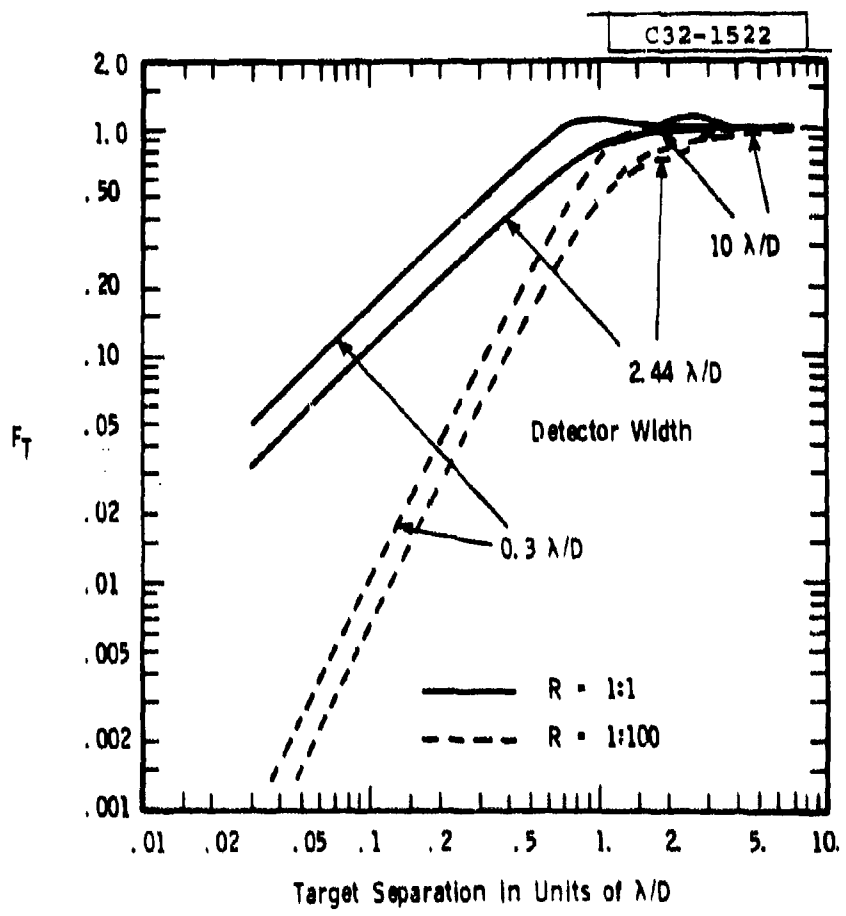


Fig. 8 Degradation of measurement precision on the target separation as a function of target separation.

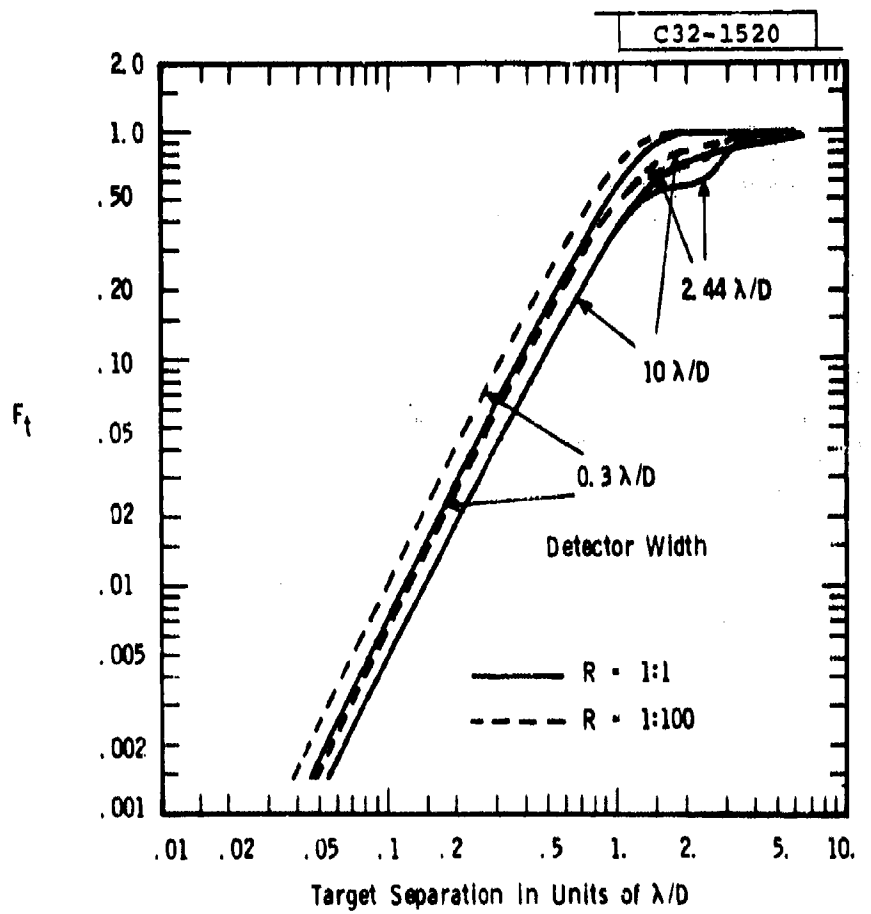


Fig.9 Degradation of measurement precision on the mid-point location as a function of target separation.

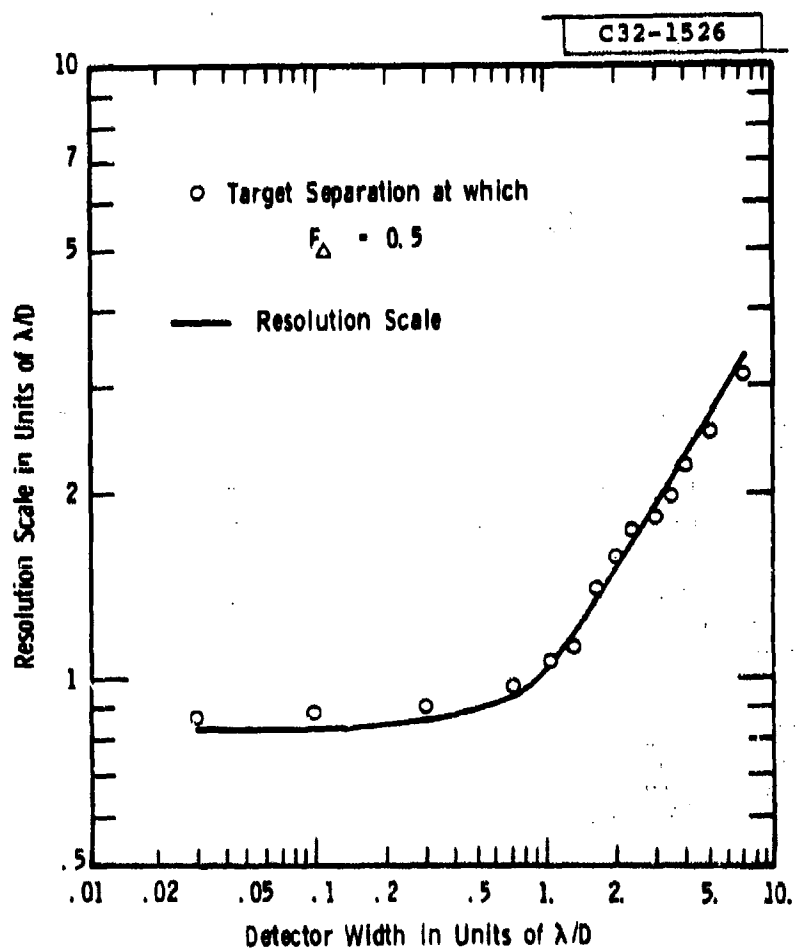


Fig.10 The resolution scale as a function of the detector width of a diffraction-limited sensor.

and the separation of the pair of objects, as well as their relative intensity are in fact equal to the associated Cramer-Rao bounds presented here.

In examining the numerical results presented here, it should be emphasized that the "optimistic" conclusion drawn by Fried is no longer true for small target separations. In some cases, when the separation is significantly less than  $\lambda/D$ , we find the numerical result presented in [1] can differ from ours as much as 3 orders of magnitude! This large deviation in the prediction of rms precision can change the conclusion regarding the capability of a particular sensor system drastically!

For separation greater than  $\lambda/D$ , the above-mentioned numerical problem seems have a very little effect on the numerical results for the prediction of rms precision. Since target separations corresponding to  $\lambda=0.5$  are in the region slightly less than to much greater than  $\lambda/D$ , Fried's major conclusion of [1] about the proposed resolution scale is still valid.

Although the results presented here are associated with a particular pulse shape, namely, a one-dimensional approximation of a two dimensional unobstructed-circular-anerture, diffraction-limited optics with a sharply delineated rectangular detector, the analytical results can be easily extended to any particular optical system, providing that the pulse shape of the output to a unit strength point source is available. The noise model considered here is an additive white Gaussian noise. For a more complicated sensor noise

model involving shot noise processes, a similar lower bound can also be obtained via the method presented in [3].

APPENDIX: CRAMER-RAO BOUND AND ERROR ANALYSIS GIVEN IN [1]

In [1], the following error covariance matrix is considered:

$$V = \text{cov}[\delta t_o, \delta T, \delta \Delta] \quad (\text{A1})$$

which is slightly different from the error covariance matrix we considered in this report. The error covariance matrix associated with the Fisher information matrix,  $F$ , is:

$$V^* = \text{cov}[\delta R, \delta T, \delta t_o] \geq F^{-1}, \quad (\text{A2})$$

where

$$R = (1-\frac{1}{2}\Delta)/(1+\frac{1}{2}\Delta). \quad (\text{A3})$$

It is easy to show that

$$V = AV^* A^T \quad (\text{A4})$$

where

$$A = \begin{bmatrix} 0 & 0 & 1 \\ 0 & 1 & 0 \\ -(1+\frac{1}{2}\Delta)^2 & 0 & 0 \end{bmatrix}. \quad (\text{A5})$$

Therefore, the Fisher information matrix associated with the error covariance matrix  $V$  becomes

$$J = A^{-T} \bar{F} A^{-1}. \quad (A6)$$

Substituting Eqs. (11a)-(11f) and (15)-(17) into (A6), the elements of  $J$  becomes:

$$J_{11} = \bar{F}_{33} = 2a^2(8\pi^2)\{[G_2(0)+G_2(T)] + \frac{1}{4}\Delta^2[G_2(0)-G_2(T)]\}/N_o, \quad (A7a)$$

$$J_{12} = \bar{F}_{23} = -2a^2(4\pi^2)\{\Delta G_2(0)\}/N_o, \quad (A7b)$$

$$J_{13} = -(1+\frac{1}{4}\Delta)^{-2}\bar{F}_{13} = -2a^2(2\pi)\{H_1(T)\}/N_o, \quad (A7c)$$

$$\begin{aligned} J_{22} = \bar{F}_{22} = 2a^2(2\pi^2)\{ & [G_2(0)-G_2(T)] + \frac{1}{4}\Delta^2[G_2(0)+G_2(T)] \\ & - 2(A_o^* A_o)\{(1-\frac{1}{4}\Delta^2)H_1(T)\}^2\}/N_o \end{aligned} \quad (A7d)$$

$$J_{23} = -(1+\frac{1}{4}\Delta)^{-2}\bar{F}_{12} = 2a^2(2\pi)(A_o^* A_o)\Delta H_1(T)/N_o, \quad (A7e)$$

$$J_{33} = (1+\frac{1}{4}\Delta)^{-4}\bar{F}_{11} = 2a^2(A_o^* A_o)[1-G_0(T)][1+G_0(T)]/N_o. \quad (A7f)$$

where we have used the following identity:

$$\bar{F}_o^{-1} = [(1+\frac{1}{4}\Delta^2) + (1-\frac{1}{4}\Delta^2)r(T)]^{-1}/(4N_o) = (A_o^* A_o)/(2N_o) \quad (A8)$$

and  $(A_o^* A_o)$  is defined in Eq. (13) of [1]. Notice that the J matrix is differed from the S matrix given in the Appendix of [1] (Eqs. (A.17)-(A.22)) by a constant, namely

$$J_{ij} = -\frac{2a^2}{N_o A_o} S_{ij} \quad \text{for all } i, j. \quad (\text{A9})$$

If we compare the  $(i,j)^{\text{th}}$  element of M matrix of [1] (Eqs. (43a)-(43f)) with  $S_{ij}$ , we find that

$$M_{ij} = -N_o A_o^* S_{ij} \quad \text{for all } i, j. \quad (\text{A10})$$

Rewriting Eqs. (39a)-(39c) of [1] in terms of matrix notation, we actually have the following expression

$$V = DMD^T \quad (\text{A11})$$

where D is the inversion of S. Applying the relationship we find in (A10), (A11) becomes

$$V = -N_o A_o^* S^{-1}. \quad (\text{A12})$$

Substituting (A9) into (A12), we finally have

$$V = -\frac{2a^2 A_o^*}{A_o} J^{-1}. \quad (\text{A13})$$

We have shown the covariance matrix  $V$  obtained in [1] for the error analysis equals to the associated Cramer-Rao bound,  $J^{-1}$ , by a constant  $2a^2 A_o^*/A_o$ . It becomes obvious that the degradation factor (a ratio of two CRB's)  $F_\Delta$ ,  $F_T$  and  $F_t$  derived from [1] and current analysis should be identical.

ACKNOWLEDGMENTS

The author would like to thank Dr. M. J. Tsai for many fruitful discussions and also Drs. John Tabaczynski, Steve Weiner and C. B. Chang for their critical comments and careful reviews. The author also wished to thank Frances Chen for her programming assistance. In addition, the skillful typing of the manuscript by C. A. Lanza is most appreciated.

### REFERENCES

1. D. L. Fried, "Resolution, Signal-to-Noise Ratio and Measurement Precision," Optical Science Consultants, Report No. TR-034, (October 1971), also published in J. Opt. Soc. Am., 69, 399 (1979).
2. R. W. Miller, "Accuracy of Parameter Estimates for Unresolved Objects," Technical Note 1978-20, Lincoln Laboratory, M.I.T. (8 June 1978), DDC AD-B028168.
3. M-J. Tsai and K-P. Dunn, "Performance Limitation on Parameter Estimation of Closely Spaced Optical Targets Using Shot-Noise Detector Model," Technical Note 1979-35, Lincoln Laboratory, M.I.T. (13 June 1979).
4. M-J. Tsai and K-P. Dunn, "Comparison of Two Detector Models for the Study of CSO Resolution Problem," Lincoln Laboratory, M.I.T., not generally available.
5. J. R. Sklar and F. C. Schweppe, "The Angular Resolution of Multiple Targets," Group Report 1964-2, Lincoln Laboratory, M.I.T. (14 January 1964), DDC AD-430185.
6. G. E. Pollon and G. W. Lank, "Angular Tracking of Two Closely Spaced Radar Targets," IEEE Trans. Aerospace Electron Systems, AES-4, 541 (1968).
7. H. L. Van Trees, Detection, Estimation and Modulation Theory, Part I, (Wiley, New York, 1968).

UNCLASSIFIED

**SECURITY CLASSIFICATION OF THIS PAGE (When Data Entered)**

**DD FORM 1473 EDITION OF 1 NOV 65 IS OBSOLETE**  
1 JAN 73

**UNCLASSIFIED**

**SECURITY CLASSIFICATION OF THIS PAGE (When Data Entered)**